



Fast non-rigid points registration with cluster correspondences projection

Minqi Li^{a,b}, Richard Yida Xu^b, Jing Xin^c, Kaibing Zhang^{a,*}, Junfeng Jing^a

^a School of Electronics and Information, Xi'an Polytechnic University, Xi'an 710048, China

^b Faculty of Engineering and Information Technology, University of Technology, Sydney, PO Box 123, Broadway Sydney, NSW 2007 Australia

^c Faculty of Automation and Information Engineering, Xi'an University of Technology, Xi'an 710048, China



ARTICLE INFO

Article history:

Received 17 July 2019

Revised 31 October 2019

Accepted 8 December 2019

Available online 19 December 2019

Keywords:

Non-rigid registration

Cluster correspondences projection

Deformation estimation

ABSTRACT

In this paper, we propose a fast non-rigid points registration method based on cluster correspondences projection. Firstly, a distance based clustering method is applied on the large scale points clouds. Then, the cluster centers are extract to represent the shape of the template and target object. After that, the target and template data are efficiently registered by an EM-like non-rigid registration method with a clustering projection between the cluster centers and all the points in the clusters. To more improve the computation efficiency, a fast deformation estimation is applied in reproducing kernel Hilbert space. As the size of cluster centers is much less than the size of the original point cloud and the cluster correspondences projection well keeps the points deformed smoothly in the clusters, the proposed method is robust and extremely efficient for large scale points registration with rigid and non-rigid deformations without loss accuracy. Experimental results show that, the efficiency of our approach outperforms on both synthesized and real datasets than the state-of-the-art methods under various types of distortions.

© 2019 Elsevier B.V. All rights reserved.

1. Introduction

Image registration is a fundamental problem in many areas including image processing, computer vision, pattern recognition, medical image analysis and so on. By using the extracted feature points to represent the shape or original image, many tasks in these fields can be formulated as a point set registration problem [1,2].

Point set registration may consider rigid or non-rigid objects. Rigid registration aims to find a global rigid-body transformation that aligns two shapes. Various methods have been developed over the past decades. Particular, the iterative closest point (ICP) and its variant methods are very popular and successful [3–6]. Non-rigid registration is more challenging as it has to estimate a set of local transformations instead of a single global transformation, and is prone to the overfitting issue due to underdetermination [5,7]. In addition, with the development of higher resolution 2D cameras or larger range 3D sensors, more efficient registration methods robust to noise, outliers and occlusions are highly desirable in real applications.

Many existing non-rigid registration methods are considered as a probability density estimation problem, such as Gaussian Mix-

ture Models(GMMs). In general, these probabilistic approaches are able to exploit the global relationships between the neighborhoods of the point sets, when the rough structure of a point set is preserved [8]. To improve the robustness, local features [8–10], manifold regularization [11,12], neighborhood constraints [13,14], patch constraints [15] are often imposed on the non-rigid registration algorithms [2,7]. It is reasonable to prompt such constraints. As we know, the local structures among neighboring points are strong and stable, even for non-rigid objects. For example, most neighboring points on a non-rigid shape cannot move independently under deformation due to physical constraints (e.g. human bodies). Without local constraints, the noisy points and outliers often lead to a high number of false correspondences even using local feature descriptors such as shape context (SC) [9]. Particularly, when the number of outliers are large and feature descriptors are similar. Moreover, the large scale point cloud non-rigid registration is difficult in practice on ordinary computers or laptops, especially, when the point cloud corrupted by various types of noise, outliers and occlusions.

To address these issues, in this paper, we formulate the point registration as an estimation of a mixture of densities. However, Gaussian densities are constrained to coincide with point clusters, but not independent points. Cluster correspondences projection method is used to estimation the correspondences between the points and the clusters. So the local constraints in the cluster

* Corresponding author.

E-mail address: zhangkaibing@xpu.edu.cn (K. Zhang).

can be preserved during the matching process. At the same time, we estimate the transformation by a fast method in the reproducing kernel Hilbert space (RKHS). Rather than randomly select the basis vectors, we select the cluster centers as the basises which are more robust to noises and outliers.

The remainder of this paper is organized as follows. Section 2 reviews the related work of rigid and non-rigid registration methods. In Section 3, we present the details of our proposed cluster correspondences projection based method and the fast transformation estimation. In Section 4, different experimental results on three types of data are presented to show the performance of our method. Finally, in Section 5, we draw a conclusion.

2. Related work

Point registration can be roughly categorized as rigid or non-rigid depending on the underlying transformation model.

For rigid registration, Iterative Closest Point (ICP) based algorithms and variants are the most popular methods. This kind of methods iteratively find the closest points for correspondences and use them to solve the optimal transformations [16]. A naive implementation of ICP is known to be sensitive to noises, outliers, and initializations for avoiding local convergence problem [17,18]. Many variants on the original ICP approach have been proposed, including generalized ICP [4], global ICP [19,20], and so on [7,21]. However, most of the ICP related methods consider the global deformation of the whole point sets. It is no longer valid in the case of non-rigid transformation with local deformations, especially when the deformation is large [22,23].

For non-rigid point registration, many existing non-rigid registration methods consider the alignment of two point sets as a probability density estimation problem, such as GMM. Expectation Maximization (EM) method is often used to solve the mixture models, and Thin Plate Splines (TPS) is applied to build the transformation model for non-rigid transformations. It is a reasonable assumption for the non-rigid registration problems as points from the template set are distributed with a certain probability distribution (such as Gaussian distribution) around points belonging to the target set. Tsin and Kanade [24] proposed a kernel correlation (KC) based point matching approach in the form of kernel density estimates. Jian and Vemuri derived a closed-form expression for the L2 distance between two Gaussian mixtures to improve the registration efficiency [25]. Ma et al. applied a L2E estimator for estimating the transformation to improve the robustness [26]. Particularly, Chui and Rangarajan developed a general framework called TPS-RPM [22]. They introduced soft assignments and solve it in a continuous optimization framework involving deterministic annealing algorithm. Other researchers utilized an asymmetric Gaussian representation for the non-rigid point set registration problem under the framework of TPS-RPM, which is robust to a large degree of degradation [27,28]. Recent researches also focus on deep learning based methods for image registration problems. Convolutional neural networks (CNN) are applied to extract the features or estimate the deformation instead of TPS [29–32]. For example, the deformation estimation is considered as a linear regression problem based on CNN regressors [33]. However, it is only specifically optimized for a certain class of images [29] and requires a large set of training pairs for different deformations [31,32]. Deep learning based methods have not been proved the efficiency in large deformed point data sets.

On the other hand, different strategies have been used to prompt the robustness. Specifically, Laplace regularizations or manifold regularization is used to preserve the intrinsic geometry of the point set, leading to a better estimation of the transformation [11,34–36]. Local features are also used to keep local con-

straints such as shape context [8,9,37], FPFH [10]. One drawback of these approaches is that neighboring points in one shape may be matched to two points far apart in the other shape [13]. Besides, Pathak et al. presented a robot-pose-registration algorithm, which is entirely based on large planar-surface patches extracted from point clouds [15]. Unfortunately, it is more suitable for rigid registration. Moreover, although patches based or clusters based method has been used for non-rigid registration, they are more concerned for keeping the robustness but not converging speed.

Another challenge for non-rigid registration is reducing the computational complexity when handling large scale data sets. To improve converging efficiency, Lian and Zhang [38] showed that the energy function of RPM can be reduced to a concave function with very few non-rigid terms, which facilitates the use of large scale optimization techniques. Ma et al. used a sparse approximation to achieve a fast implementation for transformation estimation in RKHS [8]. Myronenko et al. use the Gaussian radial basis function (GRBF) to build the transformation model instead of the TPS for nonrigid transformations for handling a large number of points with fast Gaussian transformation [39]. These strategies can partly improve the efficiency. However, most of the present models, like GMM, every point is seen as a probabilistic distribution and the distance is defined as the correlation of two densities. It needs to estimate the underlying number of Gaussian components. When the number of points is large, this may cause significant heavy computations. Lian et al. presented a quadratic programming based cluster correspondence projection (QPCCP) algorithm to reduce the computational cost [40]. A point clustering technique is introduced and the projection is conducted on the clusters instead of the original independent points. However, the accurate performance is moderate.

In this paper, we propose a fast non-rigid registration method based on cluster correspondences projection. Firstly, a clustering method is applied on the large scale cloud points. We show that the object shapes can be well presented by graphs constructed by cluster centers. Then, the target and template data are efficiently registered by an EM-like non-rigid registration method with a cluster correspondences projection between the clusters and all the points in the clusters. Finally, a fast method for deformation estimation is applied in RKHS. The performance of our proposed method will be verified on three different dataset.

3. Proposed method

Suppose there are two point sets to match: the template data points $X = \{\mathbf{x}_i, 1 \leq i \leq m\} \in R^{d \times m}$ and the target data points $Y = \{\mathbf{y}_j, 1 \leq j \leq n\} \in R^{d \times n}$, where m, n are the numbers of points, and d is the dimension. The goal is to estimate a matching matrix P between X and Y , and the transformation function f , which warps the template points X to the target points Y . By the well-known framework in [22], the points registration problem is formulated as a GMM, where the observed data \mathbf{y}_j is assumed either to be sampled from a Gaussian distribution as a correspondence point in X , or a uniform distribution as an outlier. Traditionally, the number of mixed Gaussian distributions is m , which equals to the number of the template points. Let $Z = \{z_j\}_{1 \leq j \leq n}$ represents the assignments of \mathbf{y}_j to a Gaussian distribution with zero mean and σ^2 variance, and $z_j = m + 1$ to be an outlier. The likelihood for \mathbf{y}_j with a correspondence \mathbf{x}_i in the template is $P_{ij} = P(\mathbf{y}_j|z_j = i) = \mathcal{N}(\mathbf{y}_j|f(\mathbf{x}_i), \sigma^2)$, $\forall i, 1 \leq i \leq m$. The likelihood of an observation given its assignment to the outlier is $P(\mathbf{y}_j|z_j = m + 1) = \mathcal{U}(\mathbf{y}_j|a)$, where $\mathcal{U}(\cdot)$ is a uniform distribution with a parameter a . We have the following mixture density model:

$$P(\mathbf{y}_j|\theta) = \sum_{i=1}^m (1 - \gamma) \frac{\pi_{ij}}{(2\pi\sigma^2)^{d/2}} e^{-\frac{\|\mathbf{y}_j - f(\mathbf{x}_i)\|^2}{2\sigma^2}} + \gamma \frac{1}{a}, \quad (1)$$

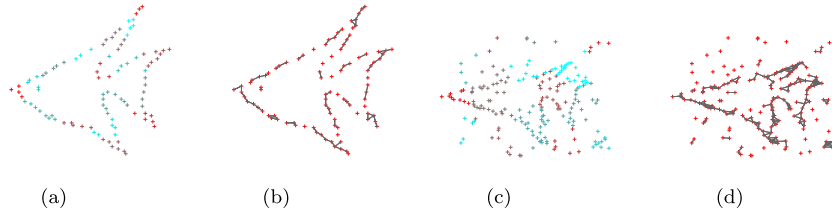


Fig. 1. Examples of clusters and graphs for 2d points.

where $\sum_{i=1}^m \pi_{ij} = 1$ are mixture weights. We denote $\theta = \{\sigma^2, \gamma, f\}$ the set of unknown parameters, where $\gamma \in [0, 1]$ is the percentage of outliers. By using Bayes rule, we estimate

$$\theta^* = \operatorname{argmax}_{\theta} P(\theta|Y) = \operatorname{argmax}_{\theta} P(Y|\theta)P(f).$$

This is equivalent to minimizing the negative log posterior

$$L(\theta|Y) = -\sum_{j=1}^n \ln P(\mathbf{y}_j) - \ln P(f). \quad (2)$$

To optimize the objective function (2), using an EM algorithm, the complete-data posterior is given by [8]:

$$\begin{aligned} Q(\theta, \theta^{old}) &= \frac{1}{2\sigma^2} \sum_{i=1}^m \sum_{j=1}^n P(z_j = i|\mathbf{y}_j, \theta^{old}) \\ &\cdot \|\mathbf{y}_j - f(\mathbf{x}_i)\|^2 + \frac{N_p d}{2} \ln \sigma^2 + \frac{\lambda}{2} \phi(f) \\ &- N_p \ln(1 - \gamma) - (n - N_p) \ln \gamma, \end{aligned} \quad (3)$$

where $N_p = \sum_{i=1}^m \sum_{j=1}^n P(z_j = i|\mathbf{y}_j, \theta^{old}) \leq n$.

From Eq. (1), we can see that the number of Gaussian distributions mixed is as large as the number of template points in X , and each point in Y is independent to others. However, this traditional GMM with m Gaussian means here may pose serious computation burden when the number of points m is large. To relieve the heavy computation and prompt the robustness, we consider cluster constraints for the non-rigid registration problem.

There are two main advantages of using the cluster constraints here. Firstly, although the absolute distance between the template and target points may change significantly under non-rigid deformations, the local structure between a point and its neighbors generally well preserved due to physical constraints (e.g. \mathbf{x}_i is not independent to its neighbors). Therefore, cluster constraints are benefit to keeping the local structures. As shown in Fig. 1(a) and (c), the fish data points are clustered into groups with different colors based on their positions. For better describe the local constraints in the group, we represented the groups by graphs shown in Fig. 1(b) and (d). Each point is a node in the graph and two nodes are connected by an edge if they are in the same group. When reasonably setting the clustering threshold, we can see the structure of the fish shapes can be clearly presented in the graphs. Even for the outliers existing in the fish shape, they are more likely isolated in the graph.

Secondly, when the points of X, Y are grouped by clustering, it is natural to consider all the points from one cluster are sampled from a same Gaussian distribution. Then, the number of the Gaussian distributions would be much less than the number of the points m , which will significantly improve the model's inference efficiency. The GMM model can be interpreted as a mixture model of clusters, but not points.

Assuming $\{\mathbf{x}_i\}$ is grouped into m_c clusters with indices $\{\Gamma_k^X, 1 \leq k \leq m_c\}$ and $\{\mathbf{y}_j\}$ into n_c clusters with indices $\{\Gamma_l^Y, 1 \leq l \leq n_c\}$. Here, Γ_k^X denotes the index of cluster k in X and Γ_l^Y denotes the index of cluster l in Y . Meanwhile, we can get mean cluster centers $\{\mathbf{x}_{ck}, 1 \leq k \leq m_c\}$, and $\{\mathbf{y}_{cl}, 1 \leq l \leq n_c\}$. Different clustering methods



Fig. 2. Examples of cluster correspondences projection.

can be applied here, such as K-means, farthest-point clustering. Then, similar to Eq. (1), the mixture model for the clusters takes the form:

$$P(y_{cl}|\theta) = (1 - \gamma) \sum_{k=1}^{m_c} \frac{\pi_{kj}}{2\pi\sigma^2} e^{-\|\mathbf{y}_{cl} - f(\mathbf{x}_{ck})\|} + \gamma \frac{1}{a}.$$

In this paper, we initialized π by the size of the clusters, $a = 1 - \frac{\Gamma_k^X}{\Gamma_l^Y}$, where $\{\Gamma_k^X, 1 \leq k \leq m_c\}$ denotes the index of cluster k in X , and $\{\Gamma_l^Y, 1 \leq l \leq n_c\}$ denotes the index of cluster l in Y .

Once the cluster correspondences are constructed, the points correspondences can be estimated based on the following theorem.

3.1. Cluster correspondences projection

Theorem 3.1. If $P \in C_P$, then $P_C = [q_{kl}]_{(m_c+1) \times n_c} \in C_{P_C}$, where $q_{kl} = \frac{\sum_{i \in \Gamma_k^X, j \in \Gamma_l^Y} p_{ij}}{|\Gamma_k^X||\Gamma_l^Y|} 1 \leq k \leq (m_c + 1)$ and $1 \leq l \leq n_c$. Conversely, if $P_C \in C_{P_C}$, then $P = [p_{ij}]_{(m+1) \times n} \in C_P$, where $p_{ij} = q_{kl}|_{i \in \Gamma_k^X, j \in \Gamma_l^Y} 1 \leq i \leq (m+1)$ and $1 \leq j \leq n$.

Here C_P is the constraint on the points correspondence matrix P (e.g. $\sum_{j=1}^n p_{ij} = 1$, $\sum_{i=1}^m p_{ij} \leq 1$, $p_{ij} \geq 0$, $1 \leq i \leq m$, $1 \leq j \leq n$). And C_{P_C} is the constraint on the clusters correspondence matrix $P_C = \{q_{kl}\}$ (e.g. $\sum_{l=1}^{n_c} |\Gamma_l^Y| q_{kl} = 1$, $\sum_{k=1}^{m_c} |\Gamma_k^X| q_{kl} \leq 1$, $q_{kl} \geq 0$, $1 \leq k \leq m_c$, $1 \leq l \leq n_c$). More details and the proof of Theorem 3.1 is referred to the appendix of [40].

Theorem 3.1 states the relationship between the points correspondences and the clusters correspondences. More specifically, if the point correspondence P satisfies the constraint C_P , the corresponding cluster correspondence formed by averaging the elements from the same corresponding cluster will satisfy the constraint C_{P_C} . Conversely, the points correspondences matrix P formed by duplicating P_C 's elements in the corresponding cluster will satisfy the constraint C_P .

Fig. 2 is an example of cluster correspondences projection. Fig. 2(a) shows the cluster correspondences between the template cluster centers $\{\mathbf{x}_c\}$ and target cluster centers $\{\mathbf{y}_c\}$. Fig. 2(b) shows the correspondence projection between $\{\mathbf{x}_c\}$ to $\{\mathbf{y}\}$. Each cluster in X_c is constrained by multiple points in Y . Inversely, when the cluster correspondence is constructed, the cluster in Y_c is constrained by multiple points in X .

Based on [Theorem 3.1](#), the point correspondence problem estimation can be transformed to the cluster correspondence problem. Depending the centers of the clusters, we estimate the cluster correspondence by

$$q_{kl} = \frac{\pi_{kl} e^{-\frac{\|\mathbf{y}_{cl} - f(\mathbf{x}_{ck})\|^2}{2\sigma^2}}}{\sum_{k=1}^{m_c} \pi_{kl} e^{-\frac{\|\mathbf{y}_{cl} - f(\mathbf{x}_{ck})\|^2}{2\sigma^2}} + \frac{\gamma(2\pi\sigma^2)^{D/2}}{(1-\gamma)a}}. \quad (4)$$

Then, the point correspondence p_{ij} can be approximated by

$$p_{ij} = q_{kl}|_{i \in \Gamma_k^x, j \in \Gamma_l^y}, \quad (5)$$

where $1 \leq i \leq m$ and $1 \leq j \leq n$.

Following the RPM framework, which is similar to the EM algorithm, the complete-data posterior has a similar expression as [Eq. \(3\)](#).

In E-step, we find the posterior distribution of the latent variables by the current parameter values θ^{old} including λ , σ^2 and the transformation function f . The probability matrix P can be approximated by [Eq. \(4\)](#) and the projection function [Eq. \(5\)](#).

In M-step, we update θ^{new} by $\theta^{\text{new}} = \text{argmax}_\theta Q(\theta, \theta^{\text{old}})$. As the probability matrix P has been approximated by [Eq. \(5\)](#), we can take the same complete-data posterior expression as [Eq. \(3\)](#). Taking derivatives of Q with respect to γ and σ^2 , and setting them to zero, we get

$$\gamma = 1 - N_p/n. \quad (6)$$

$$\sigma^2 = \frac{\sum_{j=1}^n \sum_{i=1}^m p_{ji} \|\mathbf{y}_j - f(\mathbf{x}_i)\|}{N_p d}. \quad (7)$$

Next, we will discuss the estimation of f term in [Eq. \(3\)](#).

3.2. Transformation estimation

Considering the terms of objective function Q in [Eq. \(3\)](#), the maximization of Q with respect to f is equivalent to minimizing the following regularized risk function [11].

$$\min_f E(f) = \min_f \sum_{j=1}^n \sum_{i=1}^m P_{ji} \|\mathbf{y}_j - f(\mathbf{x}_i)\|^2 + \lambda \|f\|^2, \quad (8)$$

where μ is a fixed positive constant.

As introduced before, different methods can be used to estimate the transformation. However, most methods, like TPS and MQ (Multiquadric) are found to be most suitable when the set of correspondences is not large (fewer than a thousand) and the space variation between the correspondences is small [41]. In order to improve the efficiency, in this paper, we applied a fast approximation of f based on the clusters in RKHS.

We say \mathcal{H} is a reproducing kernel Hilbert space (RKHS) when for any $y \in \mathbf{Y}$ and $x \in \mathbf{X}$ the linear functional which maps $f \in \mathcal{H}$ to $(y, f(x))$ is continuous [42]. Our target is finding a function with minimum norm which warping a given set of points among all functions in \mathcal{H} . We begin the approximation scheme that arises from the minimization of the following energy function.

$$E(f) = \sum_{i=1}^n \|\mathbf{y}_i - f(\mathbf{x}_i)\|^2 + \lambda \|f\|_{\mathcal{H}}^2, \quad (9)$$

where λ is a fixed positive constant.

Theorem 3.2. If \hat{f} minimizes $E(f)$ in \mathcal{H} , it is unique and has the form

$$\hat{f} = \sum_{i=1}^n K(\mathbf{x}_i, \cdot) \mathbf{c}_i, \quad \text{with } (K + \lambda n I) \mathbf{c} = \mathbf{y}, \quad (10)$$

where $\mathbf{c}_i \in \mathbb{R}^d$, $\mathbf{c} = (\mathbf{c}_1, \dots, \mathbf{c}_n)$, the kernel matrix $\mathbf{K}_{ij} = K(\mathbf{x}_i, \mathbf{x}_j)$ is a $n \times n$ block matrix.

More details about the proof of the theorem and the derivation of the solution for the objective function can be referred to [42–44].

Based on the [Theorem 3.2](#), it is easy to have the optimal f in our $E(f)$ [Eq. \(8\)](#) has the similar form as [Eq. \(10\)](#) with \mathbf{c} satisfying [8]:

$$\mathbf{c} (K \text{diag}(\mathbf{1}^T \mathbf{P}) + \lambda \sigma^2 \mathbf{I}) = \mathbf{Y} \mathbf{P}, \quad (11)$$

where $K \in \mathbb{R}^{N \times N}$ is the Gram kernel matrix with the (i, j) -th element $K_{ij} = \exp\left(-\frac{\|\mathbf{x}_i - \mathbf{x}_j\|^2}{2\beta^2}\right)$, β is a positive constant, $\mathbf{1}$ is a column vector of all ones, and $\text{diag}(\cdot)$ is the diagonal matrix.

3.3. Fast implementation

Although the above theorem is conceptually simple and yields accurate results for the general non-rigid registration problem, it is often time consuming when the number of points, outliers or the deformation is large. Because it is required to compute the Gram matrix with all the elements in the template and observed points set.

Several authors have suggested using low rank or sparse approximations to the kernel matrix in order to improve the computation efficiency and avoid explicit storage of the entire kernel matrix [45]. For sparse approximations, only a subset containing k , $k \ll m$ points is selected to represent the whole points approximately as a linear combination [46]. Specifically, we have a solution of the form:

$$f(\mathbf{x}) = \sum_{i=1}^k \kappa(\mathbf{x}, \tilde{\mathbf{x}}_i) \mathbf{c}_i, \quad (12)$$

where $\tilde{\mathbf{x}}_i$ is the selected subset, κ is the kernel matrix.

Different approaches are suggested for choosing the subset for better robustness. For example, Williams and Seeger simply picked their subset randomly [47]. Smola and Schölkopf suggested a number of greedy approximation methods that reduce some measure of the difference between K and κ iteratively [45]. Traditionally, sparse models have very often been built upon a carefully chosen subset of the training inputs [48]. Although it is possible to select the basis randomly, some samples may be drawn from a vector field which contain unknown outliers or noises. As suggested by [45], we want to add the points which are centers of clusters to the basis, not points which are outliers. In this paper, it is natural to select the cluster centers \mathbf{x}_{ci} $1 \leq i \leq m_c$ ($m_c \ll m$) as the basis vectors. Then the Gram matrix is $\kappa \in \mathbb{R}^{m_c \times n}$ with the (k, j) -th element

$$\kappa_{kj} = \exp\left\{-\frac{\|\mathbf{x}_{ck} - \mathbf{x}_j\|^2}{2\beta^2}\right\}. \quad (13)$$

Therefore, we seek a solution of the form

$$f(\mathbf{x}) = \sum_{k=1}^{m_c} \kappa(\mathbf{x}, \mathbf{x}_{ck}) \mathbf{c}_k \quad (14)$$

with the coefficients $\mathbf{c} \in \mathbb{R}^{m_c \times d}$ determined by a linear system.

Then, we can update the cluster centers by the average of the new positions from $f(\mathbf{x})$. After the EM converges, the final correspondences between the original X and Y are determined by the general case of [Eq. \(4\)](#) suggested by the [8], e.g.

$$P_{lj} = \frac{\pi_{lj} e^{-\frac{\|\mathbf{y}_l - f(\mathbf{x}_j)\|^2}{2\sigma^2}}}{\sum_{j=1}^n n \pi_{lj} e^{-\frac{\|\mathbf{y}_l - f(\mathbf{x}_j)\|^2}{2\sigma^2}} + \frac{\gamma(2\pi\sigma^2)^{D/2}}{(1-\gamma)a}}.$$

The whole algorithm is summarized in [Algorithm 1](#).

Algorithm 1 Fast non-rigid points registration with cluster correspondences projection.

Input:

- template data $X = \{\mathbf{x}_i\}$ and target data $Y = \{\mathbf{y}_j\}$.

Initialization:

- Cluster X, Y and compute cluster centers $\{\mathbf{x}_{ck}\}, \{\mathbf{y}_{c1}\}$;
- initialize $\lambda, \gamma, a, \sigma^2, \pi_{kl}$;
- Construct the Gram matrix κ by Eq.13;

Repeat:

E-Step:

Compute cluster correspondences P_c by Eq.4;

Estimate points correspondences P by Eq.5;

Update P with outliers;

M-Step:

Update λ, σ^2 , by Eq.6, and Eq.7;

Update the transformation f by Eq.11 and Eq.14;

Update cluster centers $\{\mathbf{x}_{ck}\}$ by averaging cluster points;

Until Q converges;

Output:

- The transformation $f(X)$.

3.4. Computation analysis

As we only cluster the points ONCE in the beginning of the proposed FCP (fast correspondences projection) method, we only analysis the computation in the iterations. Since the proposed algorithm uses clusters instead of the original amount of points, for correspondences estimation, the computational cost is substantially reduced. To simplify the analysis, let us assume the number of points $m = n$ in the template and target data (no outliers), the complexity of correspondences estimation is $O(n^2)$ in each iteration. If cluster numbers n_c is much less than n , it becomes $O(nn_c)$.

On the other hand, the cost of the original estimation of the transformation function in RKHS is $O(mn^2 + n^3)$ mainly because of the computing of the $n \times n$ dimension kernel matrix K . The space complexity is $O(mn + n^2)$ due to the requirements of storing K and the correspondence matrix P [49]. By using the cluster-based fast approximation, the size of the kernel matrix becomes $n_c \times n_c$. Then the time complexity is reduced to $O(mnn_c + n_c^3)$, and the space complexity is reduced to $O(mn + nn_c)$.

4. Experiments

In order to evaluate the performance of our algorithm, in this section, we conducted experiments on three types of data: i) Chui-Rangarajan datasets [22]; ii) synthetic Stanford Bunny [50]; iii) 3D deformable object dataset [51].

The performance of our proposed FCP algorithm is compared with several state-of-the-art nonrigid points registration methods, CQPOCS [40], PR-GLS [8], TPS-RPM [22], CPD [52], and MR-RPM [36] which are implemented by publicly available codes. All the experiments are conducted on a Laptop with i7-8750H 2.2GHz CPU and 8G RAM under the environment of Matlab R2018a. By default, the modified Hausdorff distance is used as the error measurement between the warped template and the target [53]. Nearest neighbor clustering is used as the clustering algorithm for our FCP method.

4.1. Results on 2D points set

Firstly, we conduct the experiment on the classical Chui-Rangarajan synthesized datasets, which are widely used to test a points registration method's performance. The dataset contains two models, a tropical fish including 96 points and a Chinese character including 108 points, which are separated into two groups, i.e, template points and targets points with different degraded shapes.

We firstly load the template data X and target data Y normalized to zero mean and unit variance. Next, $\{\mathbf{x}_i\}$ and $\{\mathbf{y}_j\}$ are clustered separately with width 0.18 as an empirical value. We can get $\{\mathbf{x}_c\}, \{\mathbf{y}_c\}$. Notice, the clustering algorithm is only implemented ONCE in the beginning. We compute the cluster centers to delegate each cluster. The covariance is initialized between $\{\mathbf{x}_c\}$ and $\{\mathbf{y}_c\}$. Referring [11], Hungarian algorithm is used to initialize the cluster correspondence matrix P_c . However, the proposed FCP method is not very sensitive to the initialization.

Fig. 3 shows an example of the iterative cluster projection progress by the proposed method. The first column presents the original template (blue color) and target (red color) points. From the second to the fourth column, we see that, the blue template cluster centers are constrained locally by the neighbors of the target points. Inversely, the target centers are constrained in a similar way. The last column illustrates the final result by projecting from the clusters to the points. It can be seen that only a small set of cluster centers can well drive the whole points set warping accurately to the target shape.

Fig. 4 and Fig. 5 show more results of our method on fish and Chinese character shapes, with deformation, noise, outliers and occlusion in every two rows. For each group, the upper row is template data points and target data points. The lower row is the registration results. From the left to right, the degree of degradation is increasing. We can see that the proposed method shows good performance for all the scenarios.

To ensure a fair comparison, the full fish and Chinese character dataset are applied to all the methods. Average errors for all the methods are shown in Fig. 6 and Fig. 8. As we can see, for the deformation and occlusion test, the accuracies of the proposed method on fish shapes are competitive to other methods, and worse than PR-GLS method. This because the number of points in the original shape and the clusters are small (less than 100 and 10 respectively). The approximation by the cluster correspon-

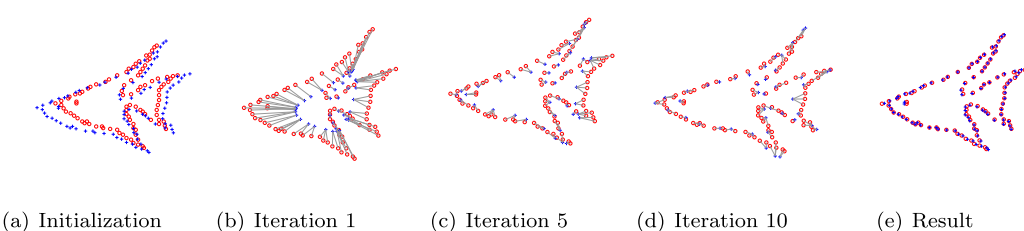


Fig. 3. Iterations of cluster correspondences projection based non-rigid points registration.

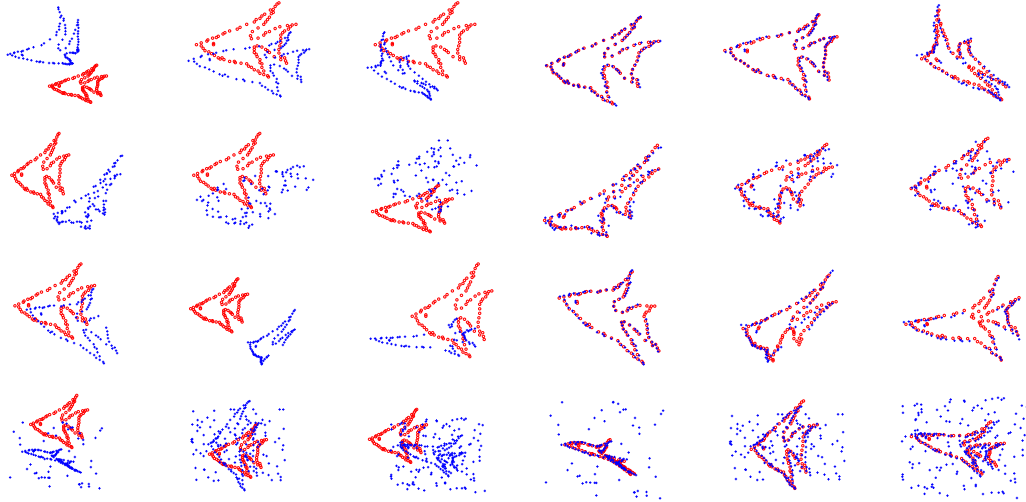


Fig. 4. Fish points registration results of our proposed method, with deformation, noise, outliers, and occlusion.

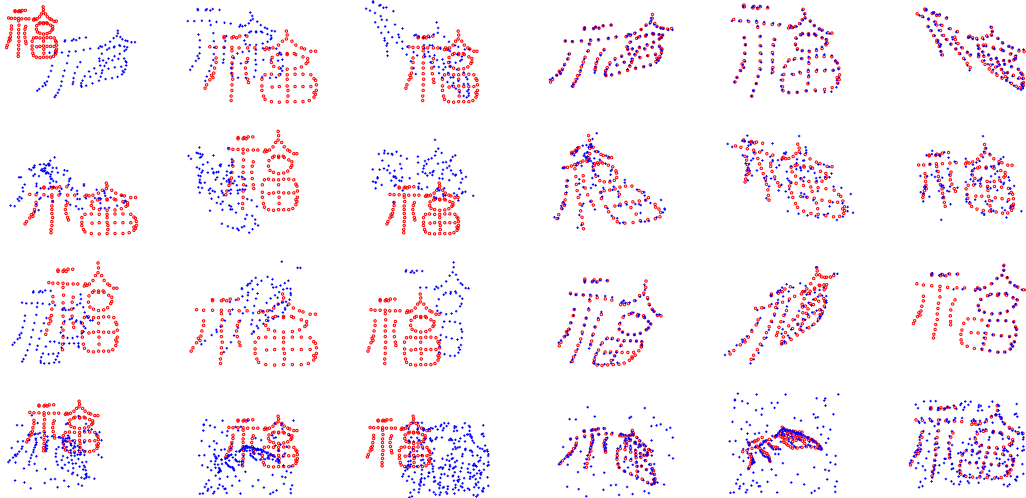


Fig. 5. Chinese character points registration results of our proposed method, with deformation, noise, outliers, and occlusion.

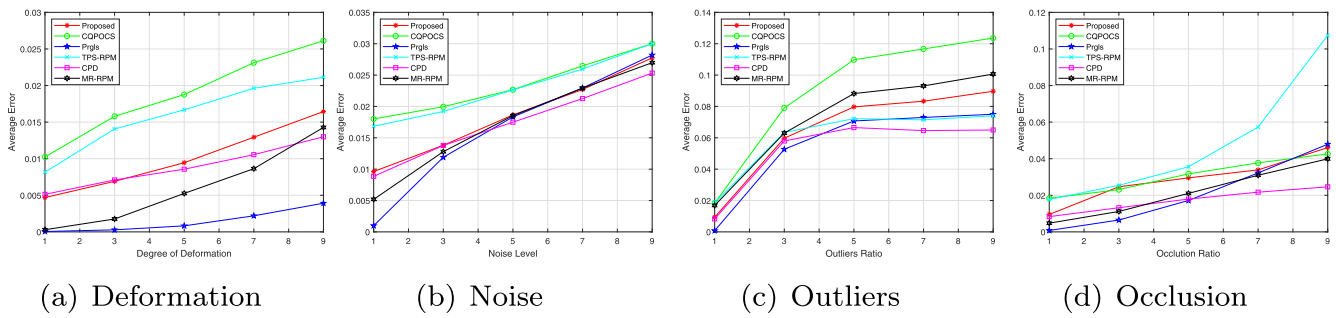


Fig. 6. Registration performance of different methods on fish dataset.

dences projection cannot fully constrain the neighbors. However, FCP method performance better on Chinese characters as the number of points increasing and the shapes are more complicated.

Similarly, although the time performances of the proposed method on both the fish and Chinese character datasets are better than other methods as shown in Fig. 7 and Fig. 9, the advantages are not obvious. This is because for small scale object shapes, the ratio between the original shape points and the number of clusters is not large (less than 4) to balance the accuracy and the speed. To

better prove the advantages of our FCP method, we will verify the results later on more large scale examples.

4.2. Results on Stanford Bunny points

To better illustrate the efficiency of the proposed method, we conduct the experiment on Stanford 3D Bunny data. We downsample the original Bunny data from 200 to 1800 points to observe the time performance on different methods. After a template point set

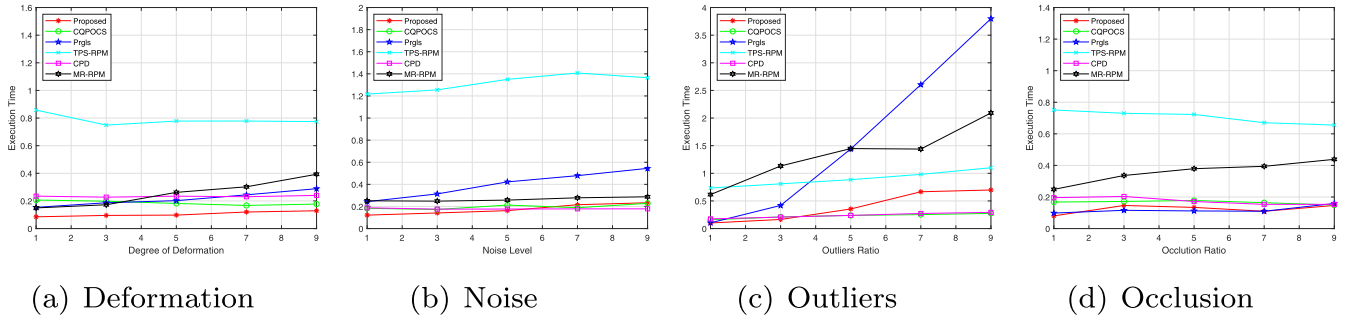


Fig. 7. Execution time of different methods on fish dataset.

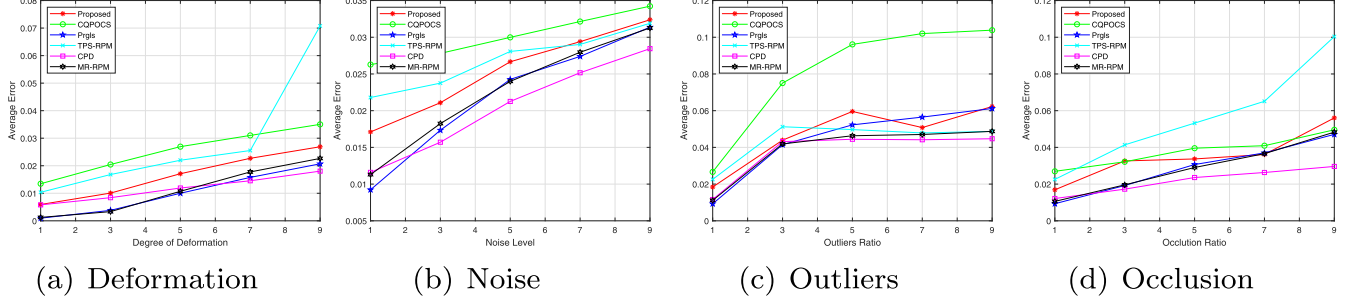


Fig. 8. Registration performance of different methods on Chinese character dataset.

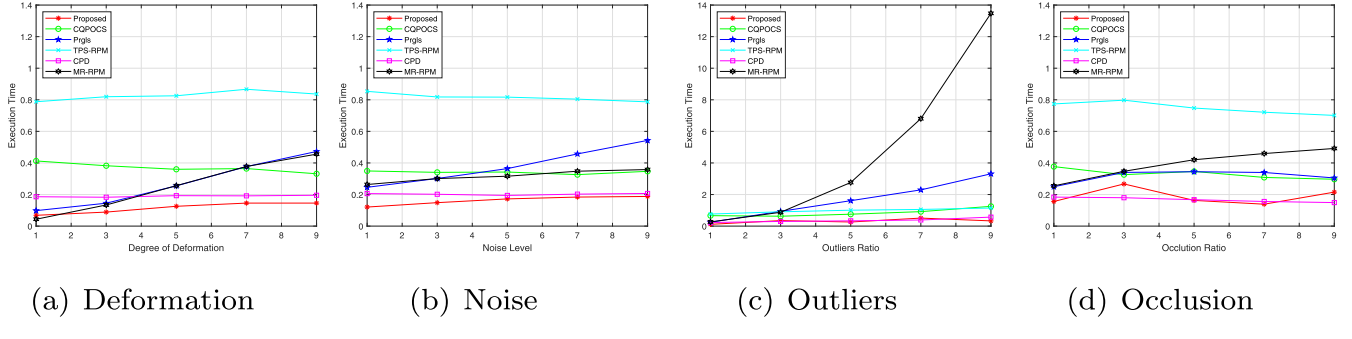


Fig. 9. Execution time of different methods on Chinese character dataset.

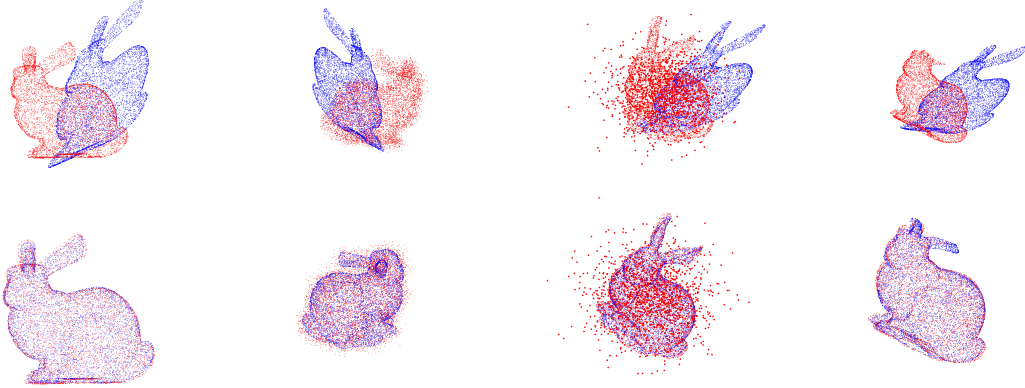


Fig. 10. Registration results on 1800 points of 3D Bunny data with deformation, noise, outliers and occlusion.

is chosen, we apply a randomly generated non-rigid transformation to warp it. Then we add Gaussian noise with 0.005 standard deviation to the warped point set to get a target point set. In the outlier test, 0.25 ratio of random outliers are added to warped data. Finally, 20 percent of occlusion points are sampled for the occlusion test.

Fig. 10 presents the registration results of the proposed method on 1800 points sampled from 3D Bunny data with deformation, noise, outliers and occlusion. The FCP method performs good at different situations. Figs. 11 and 12 show the registration errors and the time consumed by different methods. We can see that, the quality of the proposed method increases with the number of

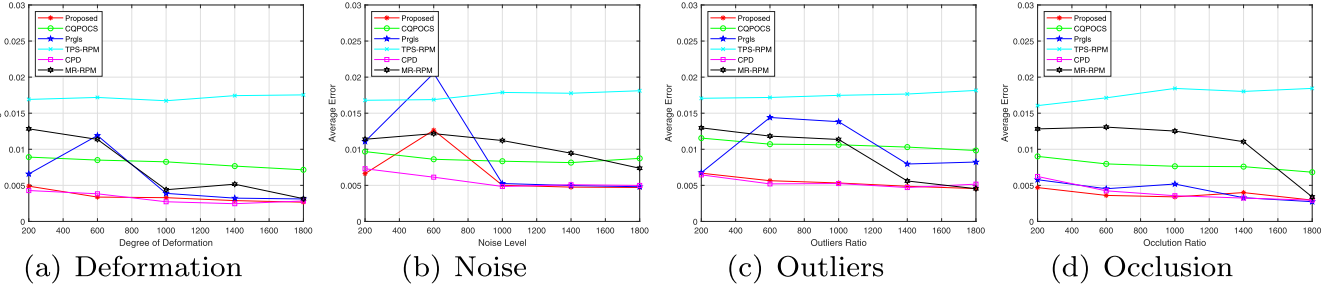


Fig. 11. Registration performance on 3D Bunny data with different number of samples.

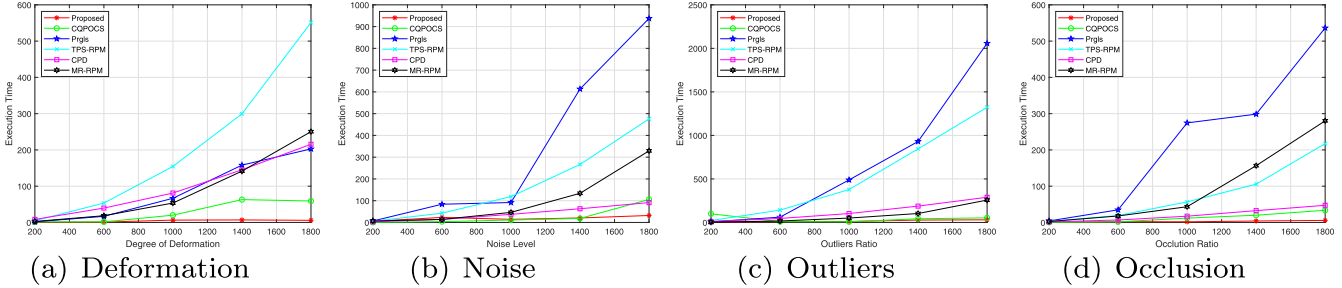


Fig. 12. Execution time on 3D Bunny with different number of samples.

the sampled points from Bunny data and presents more competitive performance than other methods when the number of sampled points is large. This is due to more clusters generated and more points clustered in one group will increase the approximation. At the same time, the time cost by PR-GLS, TPS-RPM and MR-RPM methods increases exponentially with the number of points, while the time consumed by CQPOCS, CPD methods increases linearly and more efficiently. However, compared with other methods, our proposed method shows significant efficiency. The time consuming increases linearly and slowly. It is benefited from the cluster correspondences projection and fast transformation estimation. Specifically, The cluster centers slowly increase from 135 to 216 (135, 169, 189, 213, 216) along with 200 to 1800 number of original points. For example, for the 1800 Bunny points, we cluster the data into 216 clusters. The ratio between the number of clusters and full points is about 0.1. Therefore, the correspondences computing complexity is decreased from $O(1800^2)$ to $O(0.1^2 \times 1800^2)$. Moreover, in the transformation estimation step, the deformable transformation is estimated by the fast approximation method based on the cluster centers, whose computing complexity slowly increased with the number of clusters. In addition, the transformation estimation by the cluster centers based method is more robust than the method of random selecting basis vectors. We compare the results on 1800 points of 3D bunny with 50% of outliers and $N(0, 0.01)$ Gaussian noise respectively. From Fig. 13, the number of clusters increases from 100 to 500 and the proposed cluster centers based method gives better results than the corresponding random selecting basis vectors method, especially, when the numbers of clusters are less than 300.

Different clustering methods can be used for clustering the points of Bunny, e.g. Kmean, Knn. The proposed registration method is not sensitive to different clustering methods. However, the number of the clusters greatly affects the registration speed. Table 1 shows the times cost with different number of clusters for 4000 Bunny points in the case of deformation. From Table 1 we can see that, the average errors decline slowly with the increasing number of clusters. These results are reasonable as more clusters give more accurate registration information. However, when the ratio between the number of clusters and full points is larger than

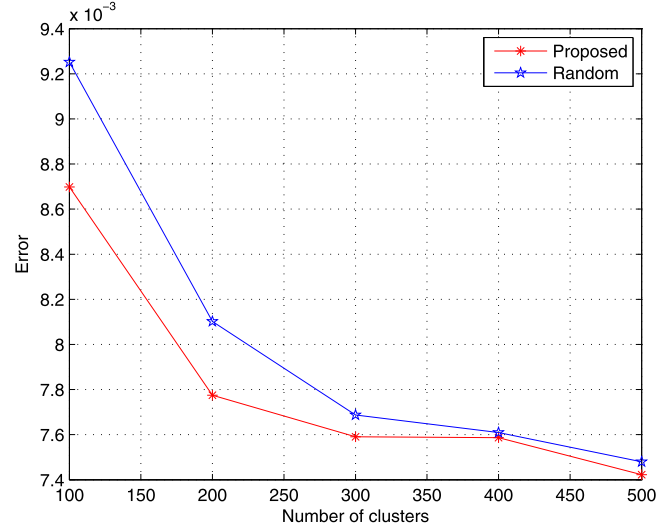


Fig. 13. Comparison of the registration accuracy by selecting bases from cluster centers and selecting bases from random samples.

0.25, the performance keeps stable. On the other hand, the time consumed increases rapidly with the increasing number of clusters. To balance the accuracy and the efficiency, it is necessary to control the ratio of the number of clusters and full points in the range of 0.1 to 0.25. Particularly, the execution time in Table 1 is including the time consumed by the clustering algorithm at the beginning.

To fully compare the results with different number of clusters and without cluster correspondences projection on different scenarios, we test the proposed method on 1500 Bunny points. Fig. 14 presents the results with different number of clusters from 150 to 750 and without cluster correspondences projection (e.g. the number of clusters equals to the number of object points). We can see that, when the ratio is above 0.25, increasing the cluster numbers wont make efficient improvement of the accuracy, while the time consuming is dramatically rising. Particularly, for the outliers and

Table 1

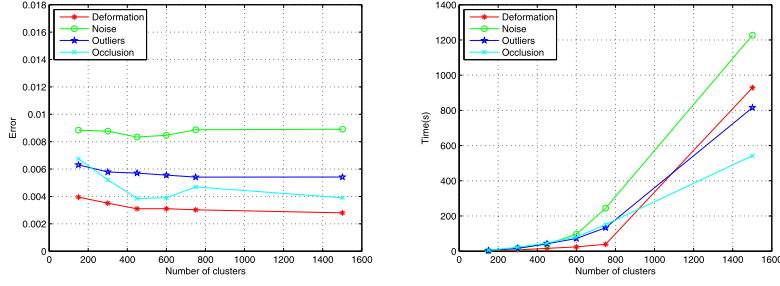
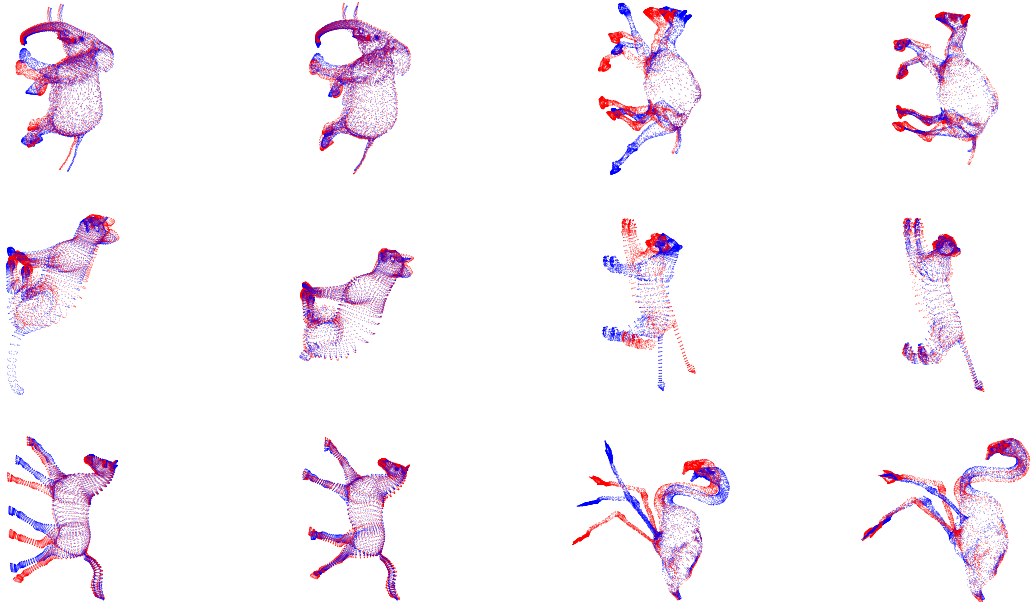
Performance of the proposed method on 4000 points of 3D Bunny with deformation by different number of clusters.

Number of clusters	100	300	500	700	900	1100
Average error	0.0037	0.0025	0.0022	0.0021	0.0020	0.0020
Execution time(s)	11.85	17.61	62.62	111.31	222.83	433.02

Table 2

Execution time of the proposed method on deformable 3D objects with thousands of points.

Point sets	elephant	cat	horse	camel	lion	flamingo
Points number	10,581	7207	8431	10,944	5000	8969
Execution time(s)	85.18	84.03	38.23	97.38	23.20	57.44

(a) Registration error with different
number of clusters(b) Execution time with different
number of clusters**Fig. 14.** Registration performance on 3D Bunny with different number of clusters and without cluster correspondences projection.**Fig. 15.** Registration results of the proposed method on deformable 3D objects with thousands of points. The first and three columns present the original template (blue color) and target (red color) points; while the second and forth columns show the registration results. (For interpretation of the references to colour in this figure legend, the reader is referred to the web version of this article.)

noise scenarios, without cluster correspondences, the registration errors are even larger.

4.3. Results on deformable 3D points set

In this section, we apply the proposed FCP method on a collection of 3D shapes from a publicly available 3D dataset, which includes seven different classes of objects (camels, cats, elephants,

horses, lions and so on) with different poses [51]. These 3D objects contain thousands of points, which are more challenging due to heavy memory and computational requirements. We select pairs of different 3D objects in the dataset, with unknown ground truth correspondences. As the compared methods cost a long time (e.g. tens of minutes, particularly, Prgls method takes hours) to complete the registrations, we only present the results and the time consuming of our proposed method as shown in Fig. 15 and

Table 2. We see that FCP can produce good alignments for different pairs, even under large deformations like camels, lions and flamingo. Surprisingly, the average running time of our FCP method on this dataset is less than 100s by a laptop with 10 thousands of points.

5. Conclusion

In this paper, we have proposed a fast non-rigid points registration method. A key characteristic of our approach is the estimation of points correspondences projected from cluster correspondences, which is robust and efficient for large scale points with different degradations. We also provide a fast implementation of deformation approximation by clusters centers in RKHS, which reduces the computational complexity significantly without reducing the quality and robustness. Experiments on public datasets for 2D and 3D non-rigid point registration demonstrate that our approach yields superior results to those of the state-of-the-art methods, especially when the scale of the points data is large.

Declaration of competing interest

The authors declare that they have no known competing financial interests or personal relationships that could have appeared to influence the work reported in this paper.

Acknowledgments

The author wishes to express the gratitude to Dr. Daniel Steinberg and the group members in DATA61, CSIRO, Sydney, Australia, for discussing the techniques about fast kernel matrix approximation for large-scale learning. This work was partially supported by the Chinese National Natural Science Foundation of China under Grant No. 61971339 and Grant No. 61471161, and the Key Project of the Natural Science Foundation of Shaanxi Province under Grant No. 2018JZ6002, and in part by the Doctoral Startup Foundation of Xian Polytechnic University under Grant BS1616 and Grant BS1726.

References

- [1] L.G. Brown, A survey of image registration techniques, *ACM Compu. Surv. (CSUR)* 24 (4) (1992) 325–376.
- [2] B. Zitova, J. Flusser, Image registration methods: a survey, *Image Vis. Comput.* 21 (11) (2003) 977–1000.
- [3] A.W. Fitzgibbon, Robust registration of 2d and 3d point sets, *Image Vis. Comput.* 21 (13–14) (2003) 1145–1153.
- [4] A. Segal, D. Haehnel, S. Thrun, Generalized-ICP, in: *Robotics: Science and Systems*, 2, 2009, p. 435.
- [5] J. Yang, K. Li, K. Li, Y.-K. Lai, Sparse non-rigid registration of 3d shapes, in: *Computer Graphics Forum*, 34, Wiley Online Library, 2015, pp. 89–99.
- [6] J. Chen, J. Ma, C. Yang, L. Ma, S. Zheng, Non-rigid point set registration via coherent spatial mapping, *Signal Process.* 106 (2015) 62–72.
- [7] G.K. Tam, Z.-Q. Cheng, Y.-K. Lai, F.C. Langbein, Y. Liu, D. Marshall, R.R. Martin, X.-F. Sun, P.L. Rosin, Registration of 3d point clouds and meshes: a survey from rigid to nonrigid, *IEEE Trans. Visualizat. Comput. Graphic.* 19 (7) (2013) 1199–1217.
- [8] J. Ma, J. Zhao, A.L. Yuille, Non-rigid point set registration by preserving global and local structures, *IEEE Trans. Image Process.* 25 (1) (2016) 53–64.
- [9] A. Thayanathan, B. Stenger, P.H. Torr, R. Cipolla, Shape context and chamfer matching in cluttered scenes, in: *Computer Vision and Pattern Recognition, 2003. Proceedings. 2003 IEEE Computer Society Conference on*, 1, IEEE, 2003, I–I.
- [10] R.B. Rusu, N. Blodow, M. Beetz, Fast point feature histograms (fpfh) for 3d registration, in: *Robotics and Automation, 2009. ICRA'09. IEEE International Conference on*, Citeseer, 2009, pp. 3212–3217.
- [11] J. Ma, J. Zhao, J. Jiang, H. Zhou, Non-rigid point set registration with robust transformation estimation under manifold regularization, in: *AAAI Conference on Artificial Intelligence*, 2017.
- [12] J.-H. Lee, C.-H. Won, Topology preserving relaxation labeling for nonrigid point matching, *IEEE Trans. Pattern Anal. Mach. Intell.* 33 (2) (2011) 427–432.
- [13] Y. Zheng, D. Doermann, Robust point matching for nonrigid shapes by preserving local neighborhood structures, *IEEE Trans. Pattern Anal. Mach. Intell.* 28 (4) (2006) 643–649.
- [14] J. Ma, J. Zhao, J. Jiang, H. Zhou, X. Guo, Locality preserving matching, *Int. J. Comput. Vis.* 127 (5) (2019) 512–531.
- [15] K. Pathak, A. Birk, N. Vaskevicius, J. Poppinga, Fast registration based on noisy planes with unknown correspondences for 3-d mapping, *IEEE Trans. Robot.* 26 (3) (2010) 424–441.
- [16] J. Paul, A method for registration of 3-d shapes, *IEEE Trans. Pattern Anal. Mach. Intell.* 14 (1992) 239–256.
- [17] Z. Zhang, Iterative point matching for registration of free-form curves and surfaces, *Int. J. Comput. Vis.* 13 (2) (1994) 119–152.
- [18] R. Horaud, F. Forbes, M. Yguel, G. Dewaele, J. Zhang, Rigid and articulated point registration with expectation conditional maximization, *IEEE Trans. Pattern Anal. Mach. Intell.* 33 (3) (2011) 587–602.
- [19] B.J. Brown, S. Rusinkiewicz, Global non-rigid alignment of 3-d scans, in: *ACM Transactions on Graphics (TOG)*, 26, ACM, 2007, p. 21.
- [20] J. Yang, H. Li, Y. Jia, Go-icp: Solving 3d registration efficiently and globally optimally, in: *Proceedings of the IEEE International Conference on Computer Vision*, 2013, pp. 1457–1464.
- [21] B. Bellekens, V. Spruyt, R. Berkvens, M. Weyn, A survey of rigid 3d pointcloud registration algorithms, in: *AMBIENT 2014: The Fourth International Conference on Ambient Computing, Applications, Services and Technologies*, August 24–28, 2014, Rome, Italy, 2014, pp. 8–13.
- [22] H. Chui, A. Rangarajan, A new algorithm for non-rigid point matching, in: *Computer Vision and Pattern Recognition, 2000. Proceedings. IEEE Conference on*, 2, IEEE, 2000, pp. 44–51.
- [23] P.J. Besl, N.D. McKay, Method for registration of 3-d shapes, in: *Sensor Fusion IV: Control Paradigms and Data Structures*, 1611, International Society for Optics and Photonics, 1992, pp. 586–607.
- [24] Y. Tsin, T. Kanade, A correlation-based approach to robust point set registration, in: *European Conference on Computer Vision*, Springer, 2004, pp. 558–569.
- [25] B. Jian, B.C. Vemuri, A robust algorithm for point set registration using mixture of gaussians, in: *Computer Vision, 2005. ICCV 2005. Tenth IEEE International Conference on*, 2, IEEE, 2005, pp. 1246–1251.
- [26] J. Ma, W. Qiu, J. Zhao, Y. Ma, A.L. Yuille, Z. Tu, Robust l2e estimation of transformation for non-rigid registration, *IEEE Trans. Signal Process.* 63 (5) (2015) 1115–1129.
- [27] G. Wang, Z. Wang, Y. Chen, W. Zhao, A robust non-rigid point set registration method based on asymmetric gaussian representation, *Comput. Vis. Image Understend.* 141 (2015) 67–80.
- [28] H. Li, T. Shen, X. Huang, Global optimization for alignment of generalized shapes, in: *Computer Vision and Pattern Recognition, 2009. CVPR 2009. IEEE Conference on*, IEEE, 2009, pp. 856–863.
- [29] K.A. Eppenhof, M.W. Lafarge, P. Moeskops, M. Veta, J.P. Pluim, Deformable image registration using convolutional neural networks, in: *Medical Imaging 2018: Image Processing*, 10574, International Society for Optics and Photonics, 2018, p. 1057405.
- [30] B.D. de Vos, F.F. Berendsen, M.A. Viergever, H. Sokooti, M. Staring, I. Işgum, A deep learning framework for unsupervised affine and deformable image registration, *Med. Image Anal.* 52 (2019) 128–143.
- [31] H. Sokooti, B. de Vos, F. Berendsen, B.P. Lelieveldt, I. Işgum, M. Staring, Non-rigid image registration using multi-scale 3d convolutional neural networks, in: *International Conference on Medical Image Computing and Computer-Assisted Intervention*, Springer, 2017, pp. 232–239.
- [32] H. Li, Y. Fan, Non-rigid image registration using fully convolutional networks with deep self-supervision, 2017 arXiv:1709.00799.
- [33] S. Miao, Z.J. Wang, R. Liao, A cnn regression approach for real-time 2d/3d registration, *IEEE Trans. Med. Imag.* 35 (5) (2016) 1352–1363.
- [34] V. Panaganti, R. Aravind, Robust nonrigid point set registration using graph-laplacian regularization, in: *Applications of Computer Vision (WACV), 2015 IEEE Winter Conference on*, IEEE, 2015, pp. 1137–1144.
- [35] G. Wang, Z. Wang, Y. Chen, Q. Zhou, W. Zhao, Context-aware gaussian fields for non-rigid point set registration, in: *Proceedings of the IEEE Conference on Computer Vision and Pattern Recognition*, 2016, pp. 5811–5819.
- [36] J. Ma, J. Wu, J. Zhao, J. Jiang, H. Zhou, Q.Z. Sheng, Nonrigid point set registration with robust transformation learning under manifold regularization, *IEEE Trans. Neural Netw. Learn. Syst.* (2018).
- [37] W. Lian, L. Zhang, D. Zhang, Rotation-invariant nonrigid point set matching in cluttered scenes, *IEEE Trans. Image Process.* 21 (5) (2012) 2786–2797.
- [38] W. Lian, L. Zhang, Robust point matching revisited: a concave optimization approach, in: *Computer Vision–ECCV 2012*, Springer, 2012, pp. 259–272.
- [39] A. Myronenko, X. Song, Point set registration: coherent point drift, *IEEE Trans. Pattern Anal. Mach. Intell.* 32 (12) (2010) 2262–2275.
- [40] W. Lian, L. Zhang, Y. Liang, Q. Pan, A quadratic programming based cluster correspondence projection algorithm for fast point matching, *Comput. Vis. Image Understand.* 114 (3) (2010) 322–333.
- [41] L. Zagorchev, A. Goshtasby, A comparative study of transformation functions for nonrigid image registration, *IEEE Trans. Image Process.* 15 (3) (2006) 529–538.
- [42] C.A. Micchelli, M. Pontil, On learning vector-valued functions, *Neural Comput.* 17 (1) (2005) 177–204.
- [43] M. Belkin, P. Niyogi, V. Sindhwani, Manifold regularization: a geometric framework for learning from labeled and unlabeled examples, *J. Mach. Learn. Res.* 7 (Nov) (2006) 2399–2434.
- [44] L. Baldassarre, L. Rosasco, A. Barla, A. Verri, Vector field learning via spectral filtering, in: *Joint European Conference on Machine Learning and Knowledge Discovery in Databases*, Springer, 2010, pp. 56–71.
- [45] R. Rifkin, G. Ye, T. Poggio, et al., Regularized least-squares classification, *Nato. Sci. Ser. Sub Ser. III Comput. Syst.* 190 (2003) 131–154.

- [46] J. Ma, J. Zhao, J. Tian, X. Bai, Z. Tu, Regularized vector field learning with sparse approximation for mismatch removal, *Pattern Recognit.* 46 (12) (2013) 3519–3532.
- [47] C.K. Williams, M. Seeger, Using the nyström method to speed up kernel machines, in: *Advances in Neural Information Processing Systems*, 2001, pp. 682–688.
- [48] J. Quinonero-Candela, C.E. Rasmussen, C.K. Williams, Approximation methods for gaussian process regression, *Large-Scale Kernel Mach.* (2007) 203–224.
- [49] J. Ma, J. Zhao, Y. Ma, J. Tian, Non-rigid visible and infrared face registration via regularized gaussian fields criterion, *Pattern Recognit.* 48 (3) (2015) 772–784.
- [50] G. Turk, M. Levoy, Zippered polygon meshes from range images, in: *Proceedings of the 21st Annual Conference on Computer Graphics and Interactive Techniques*, ACM, 1994, pp. 311–318.
- [51] R.W. Sumner, J. Popović, Deformation transfer for triangle meshes, in: *ACM Transactions on Graphics (TOG)*, 23, ACM, 2004, pp. 399–405.
- [52] A. Myronenko, X. Song, M.A. Carreira-Perpinán, Non-rigid point set registration: coherent point drift, in: *Advances in Neural Information Processing Systems*, 2007, pp. 1009–1016.
- [53] M.-P. Dubuisson, A.K. Jain, A modified hausdorff distance for object matching, in: *Proceedings of 12th International Conference on Pattern Recognition*, IEEE, 1994, pp. 566–568.



Minqi Li received a B.E. in telecommunications engineering from Xidian University, China, in 2003, and Ph.D. degree from University of Technology at Sydney (UTS), Australia, in 2016. Since 2017, he joined the College of Electrics and Information, Xian Polytechnic University, Xian, China. His current research interests include statistical machine learning and computer vision.



Richard Yida Xu received the B.E. degree in computer engineering from the University of New South Wales, Sydney, NSW, Australia, in 2001, and the Ph.D. degree in computer sciences from the University of Technology at Sydney (UTS), Sydney, NSW, Australia, in 2006. He is currently an Associate Professor with the School of Computing and Communications, UTS. His current research interests include machine learning, computer vision, and statistical data mining.



Jing Xin received the PhD degrees in control science and Engineering from Xian University of Technology, China, in 2007. She is currently a Professor with the Key Laboratory of Shaanxi Province for Complex System Control and Intelligent Information Processing, Faculty of Automation and Information Engineering, Xi'an University of Technology, Xian, China. Her current research interests main focus on manipulator robot visual servoing, mobile robot visual navigation and robust object tracking. In these areas, he has published around 50 technical articles in refereed journals and proceedings including Neurocomputing, International Journal of Advanced Robotic Systems, Sensors, Robot, etc.



Kaibing Zhang received the M.Sc. degree in Computer Software and Theory from Xihua University, Chengdu, China, in 2005 and the Ph.D. degree in Pattern Recognition and Intelligent System from Xidian University, Xian, China, in 2012, respectively. He is currently a Distinguished Professor at the School of Electronics and Information, Xian Polytechnic University, Xian, China. His main research interests include pattern recognition, computer vision, and image super-resolution reconstruction. In these areas, he has published around 30 technical articles in refereed journals and proceedings including IEEE TIP, IEEE TNNLS, Signal Processing (Elsevier), Neurocomputing, CVPR, ICIP, etc.



Junfeng Jing received the M.Sc. degree in Control Theory and Control Engineering from Xian Polytechnic University, Xian, China, in 2006 and the Ph.D. degree in Pattern Recognition and Intelligent System from Xidian University, Xian, China, in 2013, respectively. He is currently a Professor at the School of Electronics and Information, Xian Polytechnic University, Xian, China. His research interests include pattern recognition, and Machine Vision.